Modeling Electro-Mechanical Transduction In Cochlear Hair Cells

by

Asimina Courelli

Hristos Courellis

Report Supplementing our BENG 221 Presentation

Abstract

In order for the brain to perceive sound, mechanical sound waves must be converted to electrical impulses. The cochlear hair cells are responsible for detecting sound over a wide range of frequencies- 20Hz to 20,000Hz by converting sound waves into electrical impulses using stereocilia in a process called mechano-electrical transduction. The focus of this project was to develop and simulate a basic model of the mechano-electrical transduction process using a system of differential equations that model different parts of the mechano-electrical transduction system: a damped oscillator equation for the mechanical system and the cable equation for the initial stage of the propagation of the electrical signal. The solutions of these equations appear to model the basic functionality of the cochlear hair cell stereocilium, as the application of a force due to a sound wave results in spatiotemporal depolarization along the stereocilium.

Introduction

In the process of human audition, a crucial step is the conversion of longitudinal sound waves, which are picked up by the outer ear, to electrical impulses (Fig. 1A), that can be processed by the brain. The structure responsible for this mechano-electrical transduction (conversion of a mechanical stimulus to an electrical impulse) is the cochlea [2] (Fig. 1B). The cochlea is a curled, snail-like tube in the inner ear, which is comprised of a basilar membrane, surrounding fluid, the oval window, and the round window. The fluid in the cochlea, the oval window, and the round window all serve to control the movement of sound waves around the basilar membrane [1]. Vibration of the stapes in the inner ear causes the vibration of the oval window at the base of the cochlea [1]. Vibration of the oval window sends fluid 'pulses' through the cochlear fluid and around the basilar membrane. Pulses are absorbed by the round window, which is also at the base of the cochlea, opposite to the round window on the other side of the basilar membrane [1]. The part of the cochlea responsible for mechano-electrical transduction is the basilar membrane using hair cells. Hair cells on different portions of the basilar membrane are capable of sensing different frequencies of sound: 20 Hz- 20,000Hz [2]. Hair cells capable of sensing high frequencies of

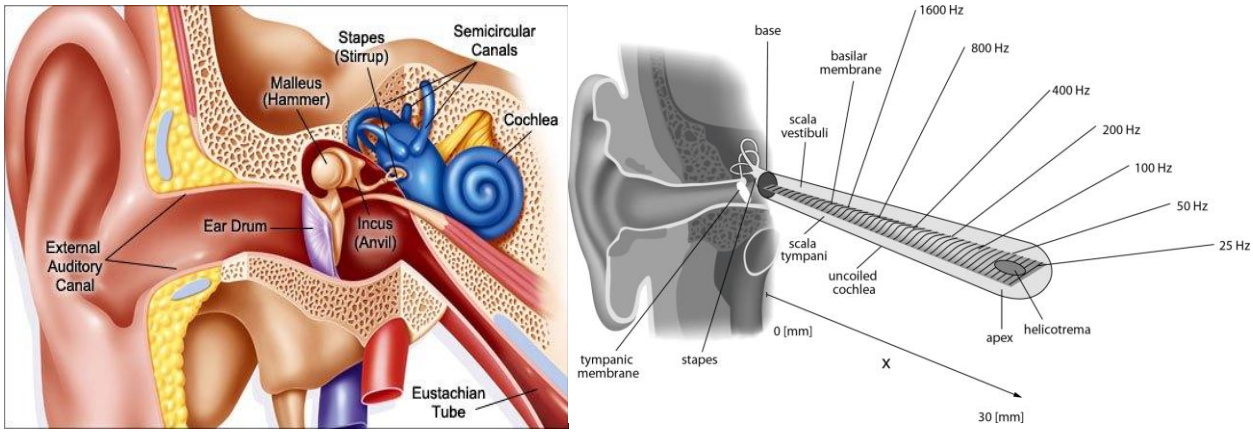

(A) (B)

Figure 1: Components of the ear responsible for capturing and transferring sound waves to the cochlea (A) and locations of the cochlea that sense different sound wave frequencies (B).

sound are located near the base of the cochlea, while hair cells near the apex sense low frequencies of sound (Fig. 1B).

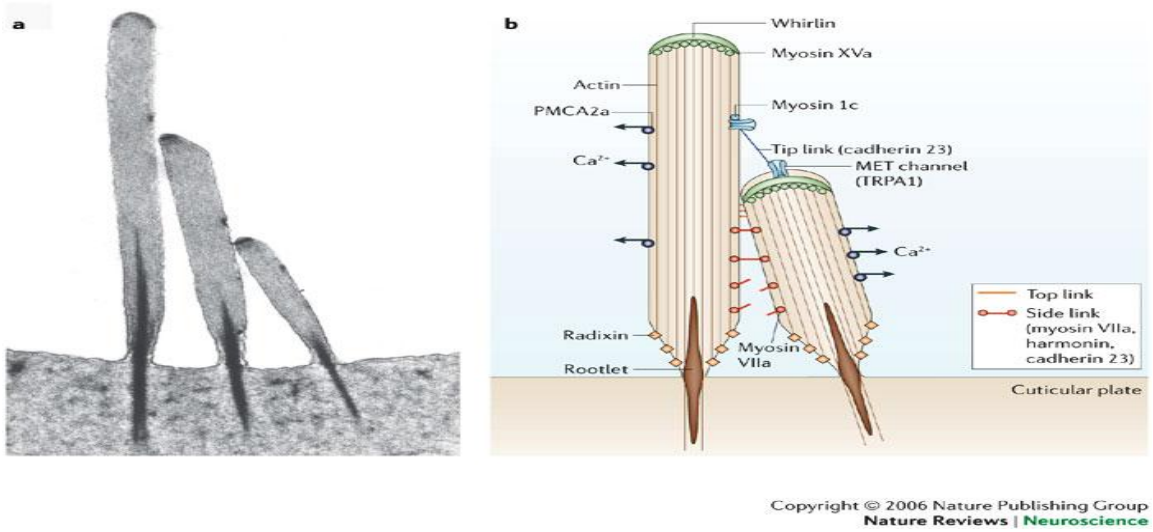

(A) (B)

Figure 2: Anatomical (A) and functional (B) picture of celial bundle.

Hair cells, the functional unit of the basilar membrane, have two main regions: 1) stereocilia and 2) cell body [1] (Fig. 2). The stereocilia are actin cylinders projecting from the cell body into the cochlear fluid. Each hair cell has multiple stereocilia (20-100) that are arranged in by height in the direction of sound propagation [2]. The stereocilia are joined at the tips by cadherins called tip links [2]. The tip links are connected to potassium channels. When a sound wave passes through a portion of the cochlea, the pressure from the longitudinal sound waves causes the stereocilia to bend [2] (Fig. 3). The stereocilial bending causes the tip links to stretch out. The tip link stretching pulls on the potassium channels located on the tip links and causes a mechanical conformation

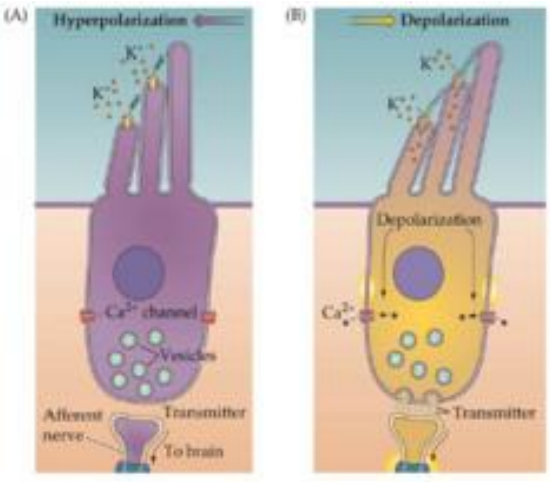

Figure 3: Sound waves cause a force to be applied to the tip. When stereocilia are bent, a mechanical conformational change is caused that leads to potassium movement into the hair cell [2].

change. This mechanical conformation change leads to potassium movement into the cell and depolarization of the stereocilial membrane [2]. The potassium current causes the opening of voltage gated calcium channels in the cell body. Depolarization in the cell body leads to neurotransmitter release onto an afferent nerve that carries the electrical impulse to the brain [1].

The focus of this project was to develop a simple mathematical model of the mechano-electrical transduction observed at the top of the stereocilia, produce an analytical solution of the model, when possible, and numerically solve the model equations to produce model responses to simple stimuli.

Methodology

There are three components to the model of mechano-electrical auditory transduction: 1) the motion of the tip link due to the bending of the stereocilia, which was modeled as a damped harmonic oscillator, 2) the influx of potassium ions into the stereocilium which was modeled as a binary static threshold function, and 3) the voltage change along the stereocilium that is caused by the initial potassium influx, which was modeled using the cable equation.

I. The Spring Equation

The equation modeling the motion of the tip link and stereocilium, when a sound wave applies a force and causes oscillation of the stereocilium, was constructed from the damped harmonic oscillator model of the tip-link/stereocilium system proposed by Fettiplace [2] (Fig. 4). In reaction to the application of a force (f_B), the stereocilium behaves like an ideal spring with a spring constant K_S. The cadherins forming the tip link also behave like an ideal spring, which is called the gating spring, with spring constant K_g, the myosin motor

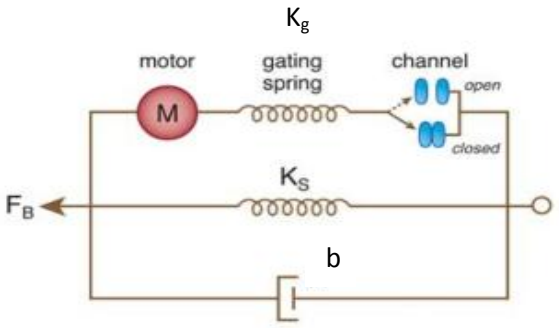

Figure 4: Diagram of stereocilium modeling as a damped harmonic oscillator from [2].

at the edges of the tip links exerts a constant force (M) in order to maintain tension in the tip links (prevent inelastic stretching of the tip links), and the dampening coefficient of stereocilial oscillation due to the inherent stiffness of the stereocilium is represented by b. In the original model, the potassium channel is considered an active component in the tip link/ stereocilium harmonic oscillator model. In fact there have been several articles (e.g., [4, 5, 6]) published on gated spring theory, where the potassium channel has varying probabilities of being open or closed based on various environmental factors. In this project, for simplicity, the dynamic involvement of the potassium channel in the oscillator system was not considered. The potassium channel was assumed to be a passive component and the solution to the differential equation, without considering the potassium channel, dictated whether the channel was open or closed. Therefore, the model shown in Figure 4 is mathematically expressed by equation 1 below. The net force experienced by the stereocilium is equal to the stereocillial mass multiplied by the net stereocilliar acceleration (Newton's 2nd law). The solution of the dampened oscillator equation is the displacement (*y*) of the stereocilium from its equilibrium point, defined as the position when the stereocilium is collinear with the cell body.

$$f_B(t) - b\frac{dy}{dt} - k_s y - k_g y - M = m\frac{d^2y}{dt^2} \qquad (1)$$

Since, initially (at t=0), the stereocilium has zero displacement and no velocity

$$y(0) = 0;\ \frac{dy}{dt}(t=0) = 0 \qquad (2)$$

Applying Laplace transform on equ.1, under the initial conditions expressed in eqs 2, we obtain:

$$F_B(s) - bsY(s) - k_s Y(s) - k_g Y(s) - \frac{M}{s} = ms^2 Y(s) \qquad (3)$$

and solving eq. 3 for *Y(s)*:

$$Y(s) = \frac{1}{\left(ms^2 + bs + \left(k_s + k_g\right)\right)} * \left(F_B(s) - \frac{M}{s}\right) \qquad (4)$$

where

$$G(s) = \frac{1}{\left(ms^2 + bs + \left(k_s + k_g\right)\right)} \qquad (5)$$

is the mechanical model's transfer function, and

$$g(t) = \mathrm{L}^{-1}\left\{\frac{1}{ms^2 + bs + \left(k_s + k_g\right)}\right\} \qquad (6)$$

its impulse response. The term

$$F_B(s) - \frac{M}{s} \qquad (7)$$

constitutes the Laplace transform of a forcing function. Then, the displacement *y(t)* can be expressed in the form of a convolution integral as follows:

$$y(t) = \int_0^\infty g(\tau) f_b(t-\tau)d\tau - M\int_0^\infty g(\tau)H(t-\tau)d\tau \quad =>$$

$$y(t) = \int_0^\infty g(\tau) f_b(t-\tau)d\tau - M\int_0^t g(\tau)d\tau \qquad (7)$$

Where *H(t)* is the Heaviside function. For an input pulse of amplitude f_0 and duration t_0 starting at *t=0* expressed by:

$$f_b(t) = f_0[H(t) - H(t-t_0)] \qquad (8)$$

the output is:

$$y(t) = f_0[\int_0^\infty g(\tau)H(t-\tau)d\tau - \int_0^\infty g(\tau)H(t-t_0-\tau)d\tau] - M\int_0^t g(\tau)d\tau \quad =>$$

$$y(t) = f_0[\int_0^\infty g(\tau)H(t-\tau)d\tau - \int_0^\infty g(\tau)H(t-t_0-\tau)d\tau] - M\int_0^t g(\tau)d\tau \quad =>$$

$$y(t) = f_0[\int_0^t g(\tau)d\tau - \int_0^{t-t_0} g(\tau)d\tau] - M\int_0^t g(\tau)d\tau \qquad =>$$

$$y(t) = f_0[\int_0^t g(\tau)d\tau - \int_0^{t-t_0} g(\tau)d\tau] - M\int_0^t g(\tau)d\tau \qquad (8)$$

II. The Ion Channel

In order for the potassium channel to open, a certain force must be applied by the tip link. In this project a static, binary behavior will be assumed, producing mechanical conformation change of the potassium channel that leads to the depolarization of the stereociliar membrane only if the stereocilium displacement is greater than a certain value $y_{threshold}$. For displacements greater than $y_{threshold}$, the tip links apply enough force on the potassium channels to drive them to an open state (probability of the channel being open is 1), allowing a potassium current I_0 to enter the cell. For displacements less than $y_{threshold}$, the tip links do not apply enough force on the potassium channels to drive them to an open state (probability of the channel being open is 0). This model assumes that there are only two possible states for the potassium channel: one in which the channel is always open and one in which the channel is always closed and is mathematically represented as follows:

$$I(y) = \begin{cases} I_0 \; if \; y > \; y_{threshold} \\ 0 \; if \; y < \; y_{threshold} \end{cases} \qquad (9)$$

I(y) shows the current into the stereocilium that is caused by the influx of potassium ions.

III. The Cable Equation

If the displacement of the stereocilium is greater than $y_{threshold}$, then the resulting current (due to potassium influx) produces a voltage change along the length of the stereocilium that can be modeled by the cable equation as follows:

$$\frac{1}{r_l}\frac{\partial^2 V}{\partial x^2} = C_m\frac{\partial V}{\partial x} + \frac{(V - V_r)}{r_m} - I(t)\delta(x - x_0) \qquad (10)$$

where V is the voltage across the stereocilium membrane, r_l is the longitudinal resistance, and the C_m and r_m the membrane capacitance and the membrane resistance respectively. V_r is the resting potential of the membrane and x is the spatial direction of the propagating voltage. The current injected into a single

spatial location x_0 at the stereocilium is represented by the term $I(t)\delta(x - x_0)$, where $\delta(x)$ is the Dirac delta function. $I(t) = I(y)$ represents the temporally varying current as it is shaped by equations (7) and (9). In this project, it is assumed that: (1) the resting membrane potential is zero, (2) the current is injected at $x_0 = 0$, (3) the flux at the boundaries ($x=0$ and $x=L$; L being the length of the stereocilial membrane) is zero, and (4) the membrane is at rest at time t=0. Thus:

$$Boundary\ Conditions:\ \frac{\partial V}{\partial x}(x = 0) = 0;\ \frac{\partial V}{\partial x}(x = L) = 0 \qquad (11)$$

$$Initial\ Conditions: V(x, 0) = V_r \qquad (12)$$

Using Green's functions, the solution of equation (10) can be written as:

$$V(x,t) = \int_0^t \int_0^L \left(G_f(x,t;\xi,\tau)I(\tau)\delta(\xi)\right]d\tau d\xi \qquad (13)$$

Since the system is LTI, equation (13) becomes:

$$V(x,t) = \int_0^t \int_0^L \left(G_f(x-\xi,t-\tau)I(\tau)\delta(\xi)\right]d\tau d\xi$$

$$= \int_0^t G_f(x,t-\tau)I(\tau)d\tau \qquad (13)$$

where $G_f(x,t)$is Green's function for the homogeneous part of equation (10) solved in the bounded interval *[0,L]*. Jackson [9] and Abbott [10] expressed $G_f(x,t)$ in terms of the infinite domain solution $G_i(x,t)$ of equation (10) as follows:

$$G_f(x,t) = 2\sum_{n=0}^{\infty} G_i(x - 2nL, t) \qquad (14)$$

where,

$$G_i(x,t) = \frac{1}{\sqrt{4\pi\frac{t}{\tau}}} e^{-\frac{t}{\tau}-\frac{\left(\frac{x}{\lambda}\right)^2}{4\frac{t}{\tau}}} * H(t) \qquad (15)$$

with *H(t)* being the Heaviside function, $\tau = C_m r_m$ and $\lambda = \sqrt{\frac{r_m}{r_l}}$.

Results

The response of the aforementioned model of the auditory mechano-electrical transduction was computed analytically and numerically for two classes of inputs: (1) a pulse input and (2) a finite duration sinusoidal input. The figures that follow show the results of these computations, which were conducted using matlab. The associated matlab scripts are included in the Appendix . The value ranges for the constants used to find the responses of the model were based on the cited literature ([2], [3], [4], [5], [7]) and were as follows: k_g (the gate spring constant) in the order of $10^{-9}\frac{N}{m}$, k_s (the stereocilia passive stiffness) in the order of $10^{-7}\ \frac{N}{m}$, b (the dampening constant) in the order of $10^{-8}\frac{Ns}{m}$, M (the myosin motor tension constant) in the order of $10^{-12}N$, m (the mass of the stereocilia) in the order of $10^{-13}kg$, I_0 (the injected current) in the order of $250\ pA$, r_l (the longitudinal resistance) in the order of $10^7\ \Omega/\text{cm}$, C_m (the membrane capacitance) in the order of $1\ \mu F/cm$, r_m (the membrane resistance) in the order of $10^{10}\ \Omega\,\text{cm}$ and L (the streocilium length) in the order of $40\ \mu m$. According to their respective references, the values of the model parameters are approximate and were chosen so as to demonstrate the temporal bandpass nature of stereociliar sensing.

First, an input pulse of amplitude 200.0 pN and duration of 40.0 ms was applied to the spring subsystem at time t=0 . The response (displacement-y) of the spring subsystem (represented by the spring equations (1) and (2)), obtained using ode23 is shown in figure 5A (blue trace) along with the output of the gating function that shapes the current injected into the stereocilium (red trace) – low (zero value)

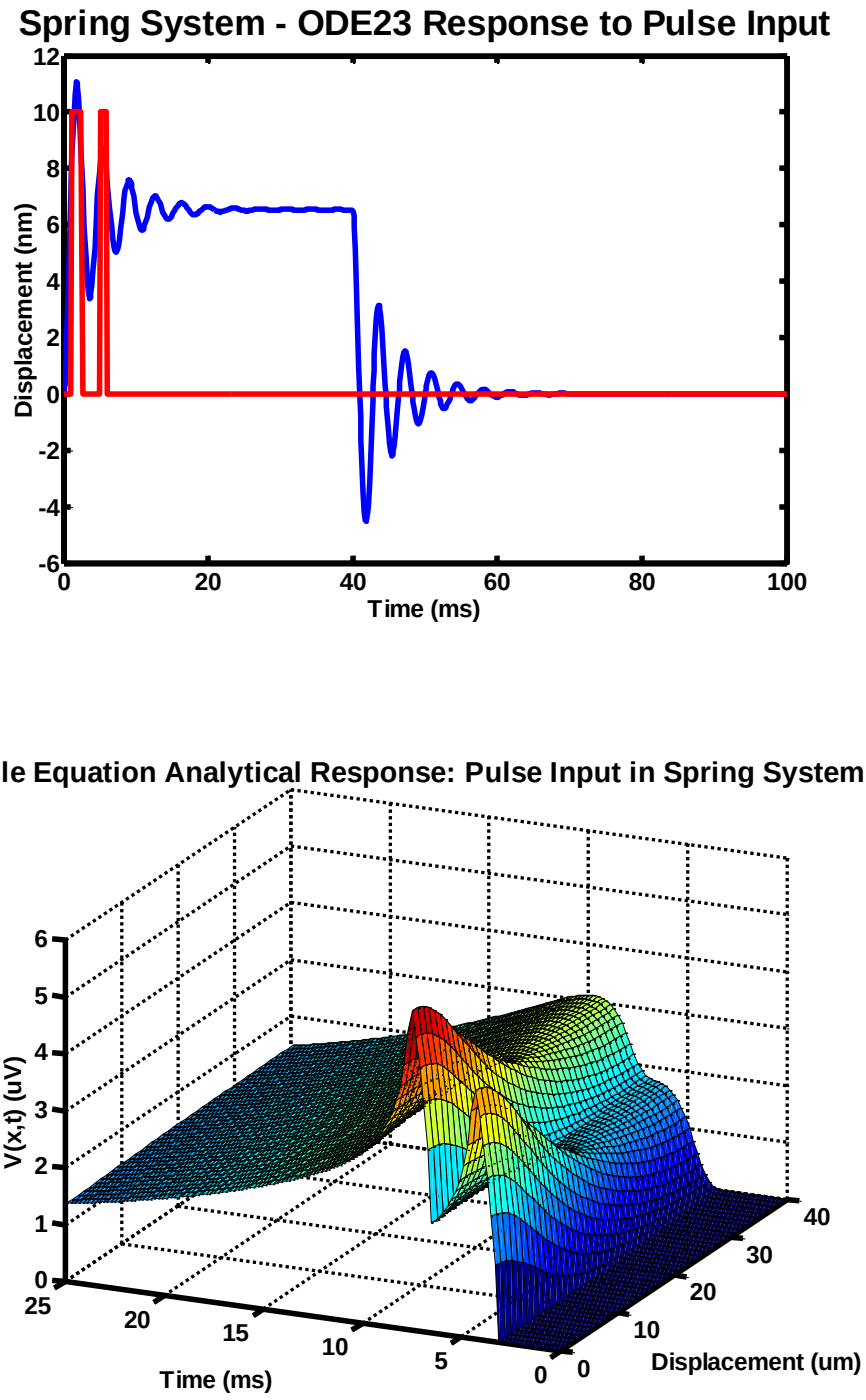

Figure 5: Response of the spring subsystem (A) and the voltage propagation subsystem (cable equation) (B) to a pulse input applied to the spring subsystem. In (A), the blue trace represents the numerical solution of the spring equation using ode 23, while the red trace indicates the points in time at which the displacement of the stereocilium is greater than the displacement threshold, allowing the influx of current. In (B), the solution of the cable equation with a forcing function shaped by the red trace from (A) is shown.

corresponds to the injection of no current while high corresponds to the injection of current. The displacement threshold value was set at 8 nm. As seen in the blue trace of figure 5A, the solution of the spring equation shows two sets of damped oscillations. The stereocilium first undergoes a short period of damped oscillation, when a force is initially applied. At 25 ms, the stereocilium reaches a steady state, at a constant displacement from the normal of about 7 nm. The constant displacement lasts until the pulse ends and there is no longer force being applied onto the stereocilium. At t = 40ms, the stereocilium undergoes a damped oscillation until it reaches steady state at 65ms.The stereocilium oscillates about the normal until it comes back to its initial, resting position. The potassium channels will only open if the displacement of the stereocilium is above a threshold level. In this case, the threshold displacement is 8 nm. As indicated by the red trace in figure 5A**,** there are two time points at which the displacement of the stereocilium exceeds the threshold level at: t~2ms and t~6ms. The red pulses indicate points in time at which the stereocilium will experience an influx of current. That is, the potassium gate is opened by the tip link and potassium flows into the cell. The incoming potassium current was modeled with a pulse of amplitude 250pA.

(A)

The solution of the cable equation (10) subject to equations (11) and (12), and a forcing function shaped by the red trace in figure 5A, using pdepe, is shown in figure 5B. For each of the two time periods corresponding to the influx of current, the stereociliar membrane experiences spatiotemporal changes in membrane voltage. At $t=0$, the membrane begins at rest with voltage of $0.0\ mV$. Considering that $x = 0$ indicates the location of the potassium channel, the most dramatic changes in membrane voltage are seen around the potassium channel, as the interior of the cell immediate to the channel should have the highest concentration of potassium ions. Any spatial change in membrane potential would be due to diffusion of potassium ions. The first influx of potassium causes the membrane potential to rapidly increase. The increase in membrane potential is, then, propagated down the sterociliar bundle, gradually attenuating as the distance increases. This behavior is shown in figure 5B by the gradual attenuation of voltage as the depth of the first rise for a given point in time is the greatest at distance $x = 0$ and decreases as distance increases. Eventually, the membrane begins to repolarize at t = 10ms. Repolarization is indicated in the graph by the decrease in membrane potential as V returns to 0 over time. Before the membrane has

(B)

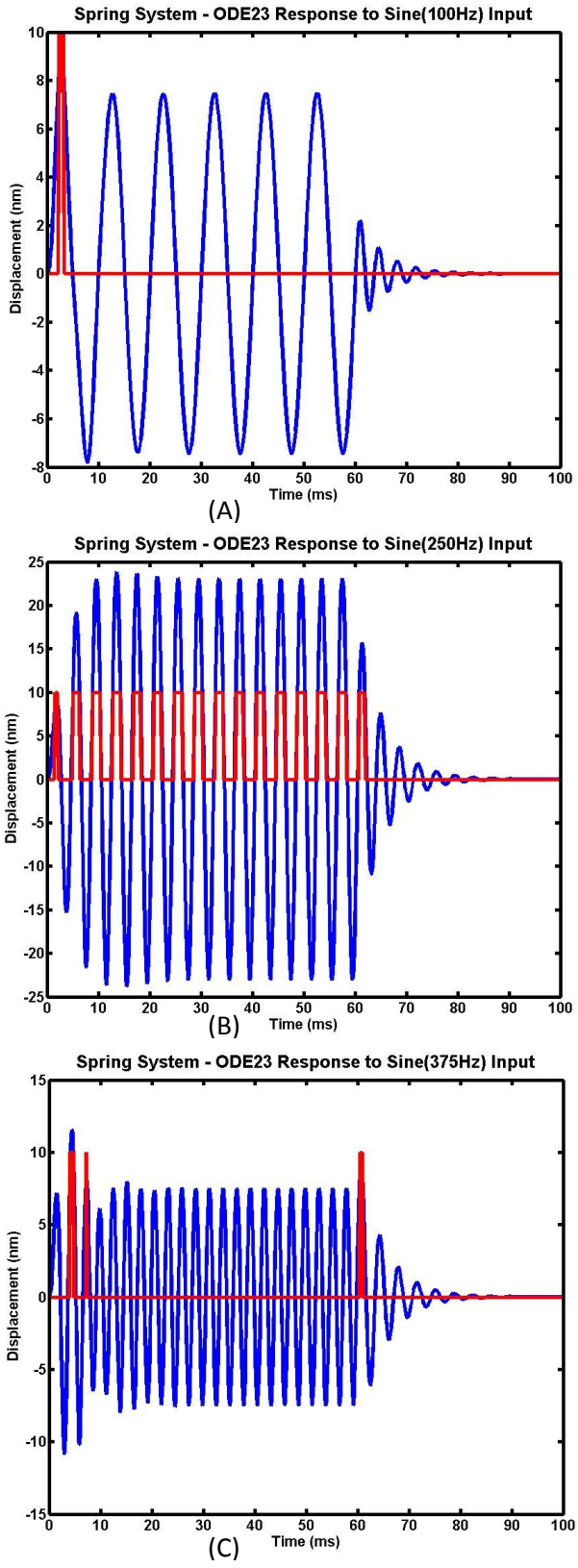

Figure 6: Numerically computed response of the spring subsystem to three sinusoidal inputs demonstrating the spring subsystem's bandpass / frequency selectivity properties. For low (A) and high (C) frequencies the response is minimal, while for frequencies in the middle (B) the response is significant.

completely repolarized, a second current pulse is delivered as the potassium channel opens again, exhibiting the same behavior as the first pulse. It should be noted that the voltage does not attenuate wit distance to 0.0 V within the length of the stereocilium. This behavior is expected as the stereocilium should deliver some voltage value to the cell at the end of its length so that the sound be sensed.

In order to more closely mimic the conditions experienced by stereocilia in a human ear, we modeled the forcing function of the spring subsystem as a sinusoidal function, since sound is more likely to take on a continuous form such as this rather than a single burst of uniform amplitude. Thus, three finite duration (60 ms) sinusoidal inputs with amplitude 200pN and frequencies of 100Hz, 250Hz, and 375Hz were applied to the spring subsystem. The corresponding responses of the spring subsystem are shown in figures 6A, 6B, and 6C respectively (blue traces). The red trace in each figure shows when the response

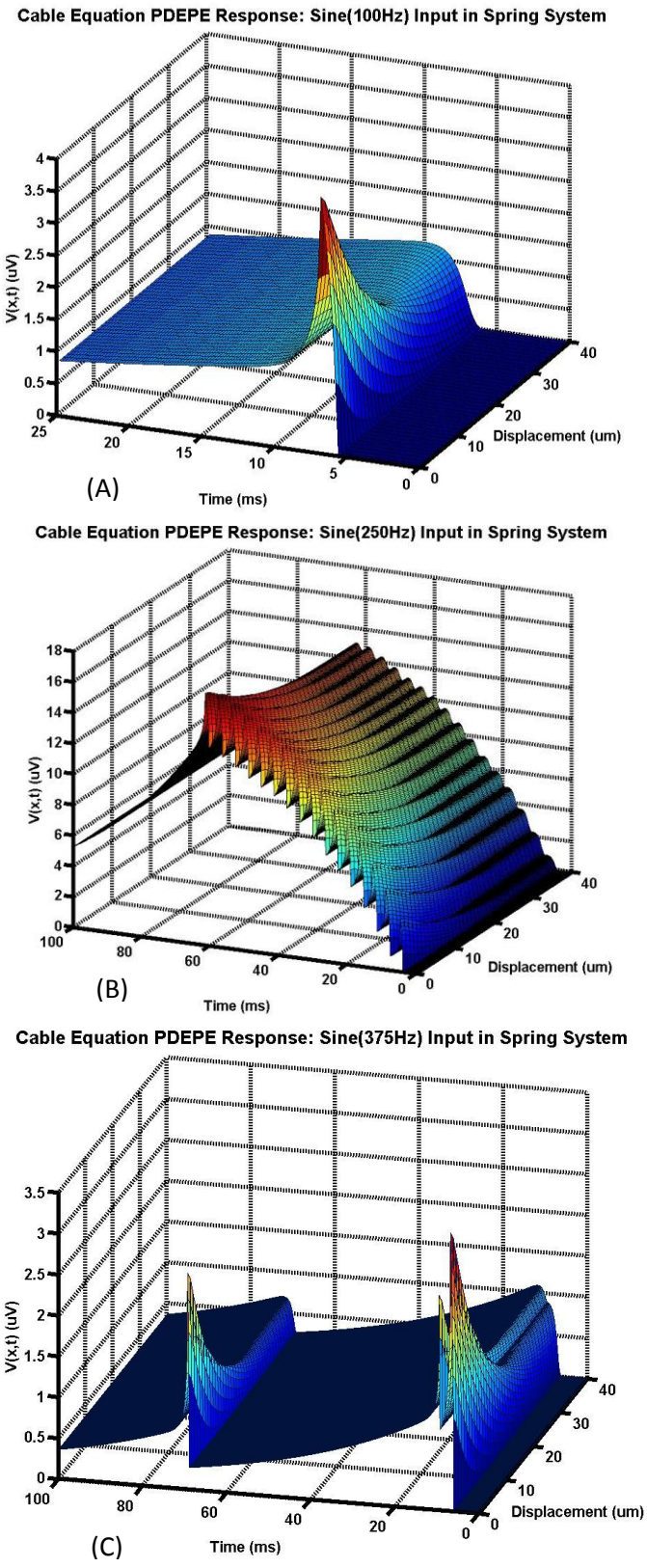

Figure7: Solution of the cable equation along the stereocilium for the three sinusoidal inputs shown in figure 6. When the stereocilium is sensitive to the frequency range of the applied force, it delivers higher voltage to the cell (B) rather when it is not (A,C)

(stereocilium displacement) exceeds the threshold value and allows potassium to enter (current influx). A comparison among the three figures reveals the bandpass property of the spring subsystem. While in the region of mid frequencies (Fig. 6B) the response of the subsystem exceeds the threshold often during the duration of the sinusoid (many red pulses) and delivers significant amounts of current, in the region of low frequencies (Fig. 6A) and high frequencies (Fig. 6C) the subsystem's response is mostly below threshold (few red pulses) and little current is delivered. The solution of the cable equation along the sterocilium for each one of these cases is shown in figures 7A, 7B, and 7C respectively. Figure 7B shows the voltage reaching a value in the order of ten times higher than the voltage in figures 6A and 6C. Thus, the stereocilium delivers to the cell higher voltage when the applied force due to oscillating sound wave is in the frequency range the stereocilium is mostly sensitive to and is designed to detect.

Figures 5, 6, and 7 provide results that have been numerically obtained by solving equations 1 and 10 using matlab's built in capability and custom scripts

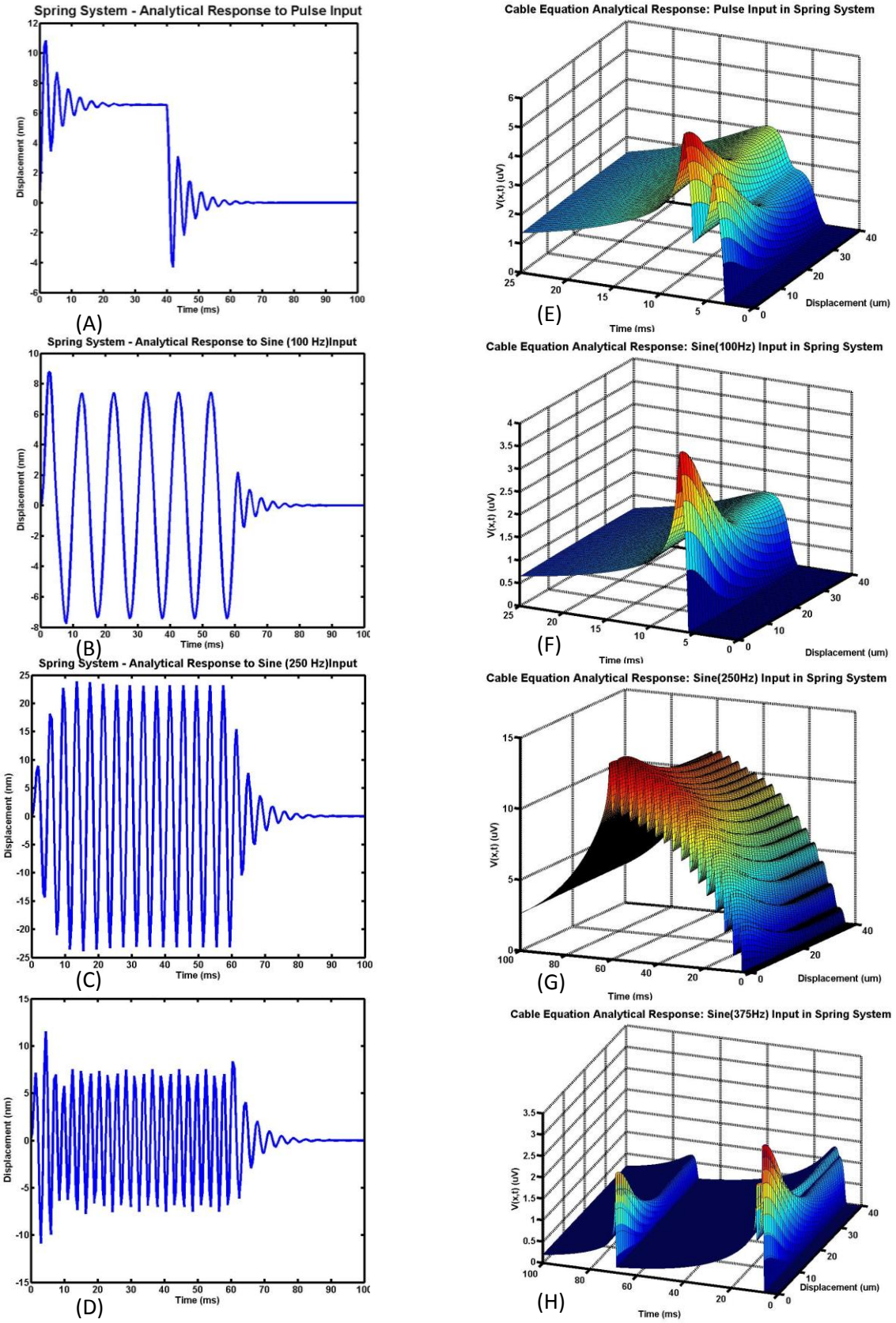

Figure 8: Graphs of the analytical solutions of equations 1(A-D) and 10 (E-F) for each of the four input cases. Comparison with their numerically computed counterparts shown in figures 5, 6, and 7 suggests very good agreement.

included in the Appendix. However, analytical solutions were also obtained for the spring subsystem (equations 7 and 8) and for the cable equation (equations 13, 14, and 15). Graphs of the analytical solutions of the spring subsystem for each of the four input cases are shown in figure 8 (A-D) and graphs of the analytical solutions for the cable equation corresponding in each of these cases are shown in figure (E-H). Comparison between the analytically and the numerically computed solutions show a very good agreement. The impulse response of the spring subsystem and Green's function for the cable equation are shown in figures 9A and 9B respectively. The shape of the impulse response of the spring system shown in figure 9A is indicative of the banpass nature of the spring subsystem. The shape of Green's function for the cable equation depicted in figure 9B shows quick temporal decay but a slower spatial attenuation, indicating quick response of the stereocilial membrane to temporal changes and limited spatial attenuation over the length of the stereocilium so that at least a fraction of produced voltage can reach the cell body.

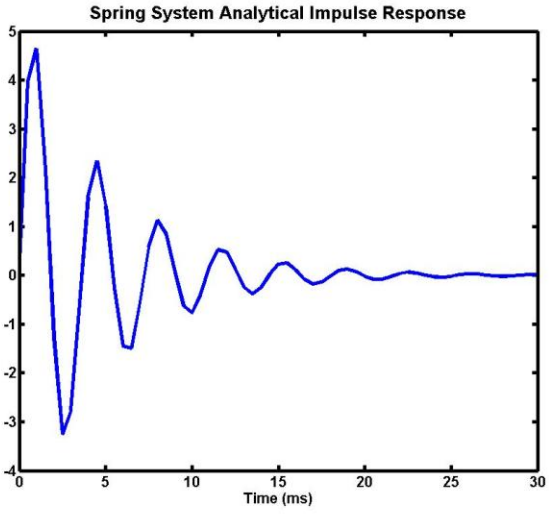

(A)

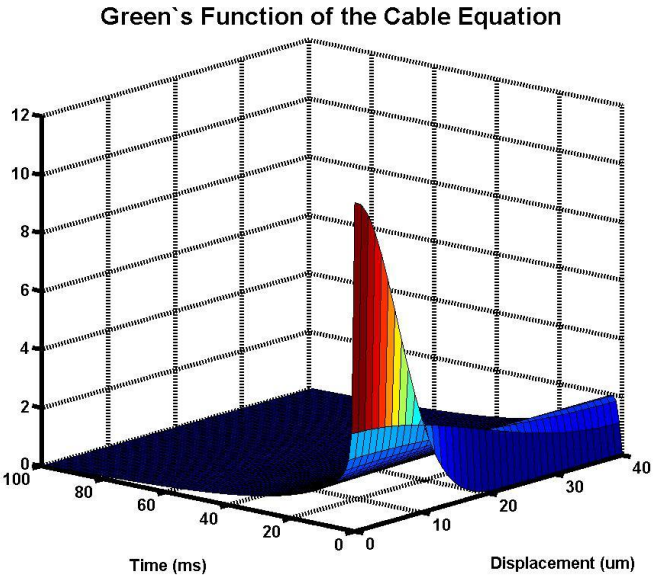

(B)

Figure 9: Graphs of the analytical expressions for the impulse response of the spring subsystem (A) and Green's function for the cable equation (B). The shape of the impulse response of the spring system (A) corroborates its banpass behavior. The quick temporal decay but the slower spatial attenuation of Green's function (B) indicate quick response of the stereocilial membrane to temporal changes and limited spatial attenuation over the length of the stereocilium.

Discussion

A simple model of the auditory mechano-electrical transduction was presented and its response to pulse and sinusoidal inputs was examined. The model constitutes an attempt to capture the functionality of a stereocilium as the force applied to it by sound waves causes a gate to open and allow potassium ions to enter, changing the voltage across the membrane and down the stereocilium up to the cell body of the hair cell the stereocilium is attached to. The mechanical portion of the stereocilium was modeled by a second order mass-spring-damper ODE, the gate was modeled by a simple static threshold function, and the propagation of the voltage down the stereocilium was modeled by the cable equation (PDE). The ODE and the PDE were solved analytically and numerically for two classes of inputs: a pulse and a finite duration sinusoid at three distinct frequencies. The values of the model parameters were selected from value ranges published in the literature.

The results of the computations indicated that the basic behavior of the auditory mechano-electrical transduction was captured, at least in principle, successfully by the model. They demonstrated the narrow frequency range specificity exhibited by stereocilia. The parameter values employed in the computations demonstrated the bandpass nature of the spring (mechanical) subsystem specific to the range between 200Hz and 300Hz. The results also demonstrated the fast temporal and the slow spatial dynamic of the voltage propagation mechanism down the stereoclium, suggesting the stereocilium's adaptability to fast temporal changes in voltage without the introduction of significant spatial attenuation that would result in delivering small voltage values to the hair cell. It should be noted that one key simplifying assumption was the non-dynamic representation of the potassium gating mechanism, although the literature reports complex dynamics governing the gating mechanism. Clearly, more extensive investigation is needed to determine the extent to and accuracy with which the model represents the auditory mechano-electrical transduction, but the fact that it does display its basic properties gives credence to the idea that a mathematically sound model was presented which successfully reproduces the basic biological dynamics of the auditory mechano-electrical transduction.

References

1. Silverthorn, Dee. *Human Physiology*. 5th ed. N.p.: Pearson, 2007.
2. Fettiplace, Robert & Kyunghee Kim. "The Physiology of Mechanoelectrical Transduction Channels in Hearing." *Physiol Rev* 94 (2014): 951-86.
3. Geisler, C. Daniel. *From Sound to Synapse: Physiology of the Mammalian Ear*. New York: Oxford UP, 1998.
4. Fettiplace, R. "Active Hair Bundle Movements in Auditory Hair Cells." *The Journal of Physiology* 576.1 (2006): 29-36.
5. Crawford, A. C., and R. Fettiplace. "The Mechanical Properties of Ciliary Bundles of Turtle Cochlear Hair Cells." *Journal of Physiology* 364 (1985): 359-79.
6. LeMasurier, Meredith, and Peter Gillespie. "Hair-Cell Mechanotransduction and Cochlear Amplification." *Neuron* 48 (2005): 403-15..
7. "2.5 Spatial Structure: The Dendritic Tree." *2.5 Spatial Structure: The Dendritic Tree*. N.p., n.d. Web. 20 Oct. 2014.
8. Gerstner, Wulfram, Werner M. Kistler, Richard Naud, and Liam Paninski. *Neuronal Dynamics: From Single Neurons to Networks and Models of Cognition*. Cambridge University Press 2014.
9. Jackson, J. D. *Classical Electrodynamics*. Wiley 1962.
10. Abbott, L. F. Realistic synaptic inputs for model neural networks. *Network*, (1991) 2:245-258.

APPENDIX: Matlab Script

```
% Plot Spring System's Impulse Response
% and Analytical Solutions

b = 4e-2;
K_s = 30e0;
M = 20e-3;
K_g = 6e-1;
m = 1e-3;
F0 = 200;

syms t;

fb1 = F0*(heaviside(t) - heaviside(t-0.4));
fb2 = F0*(heaviside(t) - heaviside(t-0.6))*sin(20*pi*t);
fb3 = F0*(heaviside(t) - heaviside(t-0.6))*sin(50*pi*t);
fb4 = F0*(heaviside(t) - heaviside(t-0.6))*sin(75*pi*t);

FB1 = laplace(fb1)
FB2 = laplace(fb2)
FB3 = laplace(fb3)
FB4 = laplace(fb4)

syms s;

 H = 1/(m*s^2+b*s+(K_s+K_g));

 h = ilaplace(H)

 Y1 = H*(FB1-M/s);
 Y2 = H*(FB2-M/s);
 Y3 = H*(FB3-M/s);
 Y4 = H*(FB4-M/s);

 y1 = ilaplace(Y1);
 y2 = ilaplace(Y2);
 y3 = ilaplace(Y3);
 y4 = ilaplace(Y4);


figure(1)
yh = subs(h,t,[0:.005:.3]);
plot([0:.5:30],yh);
Title('Spring System Analytical Impulse Response');
xlabel('Time (ms)');

figure(2)
yy1 = subs(y1,t,[0:.005:1]);
plot([0:.5:100],yy1);
Title('Spring System - Analytical Response to Pulse Input');
```

```
xlabel('Time (ms)');
ylabel('Displacement (nm)');

figure(3)
yy2 = subs(y2,t,[0:.005:1]);
plot([0:.5:100],yy2);
Title('Spring System - Analytical Response to Sine (100 Hz)Input');
xlabel('Time (ms)');
ylabel('Displacement (nm)');

figure(4)
yy3 = subs(y3,t,[0:.005:1]);
plot([0:.5:100],yy3);
Title('Spring System - Analytical Response to Sine (250 Hz)Input');
xlabel('Time (ms)');
ylabel('Displacement (nm)');

figure(5)
yy4 = subs(y4,t,[0:.005:1]);
plot([0:.5:100],yy4);
Title('Spring System - Analytical Response to Sine (375 Hz)Input');
xlabel('Time (ms)');
ylabel('Displacement (nm)');



% Plot Cable Equation's Analytical Solutions

global lambda ;
global tau ;
global ffun;
global xmesh;
global tmesh;
global el;

rlong = 1e7;
rmem = 8e10;
cmem = 5e-10;
I0 = 250e-12;
ffunp = load('ffunsavpulse');

dx=1;
dt=0.1;
x_min = 0;
x_max = 40;
t_max = 100;

lambda = sqrt(rmem/rlong);
tau = cmem*rmem;
xmesh = x_min:dx:x_max;
tmesh = dt:dt:t_max;
el = x_max;

Green = Green_fnt(1);
```

```
figure;
surf(xmesh,tmesh(1:10:end),Green(:,1:10:end)')
Title('Green`s Function of the Cable Equation');
ylabel('Time (ms)');
xlabel('Displacement (um)');

ffunp = ffunp.* (rlong*I0/max(ffunp));

ffun = resample(ffunp,length(tmesh), length(ffunp), 0);

V = zeros(length(xmesh), length(tmesh)+length(ffun)-1);
for ix=1:1:length(xmesh);
    V(ix,:)=(1e6)*dx*dt*conv(Green(ix,:), ffun, 'full')/tau/lambda;
end

figure;
surf(xmesh,tmesh(1:2:end/4),V(:,1:2:length(tmesh)/4)')
Title('Cable Equation Analytical Response: Pulse Input in Spring System');
ylabel('Time (ms)');
xlabel('Displacement (um)');
zlabel('V(x,t) (uV)');


ffuns100 = load('ffunsavs100');

ffuns100 = ffuns100.* (rlong*I0/max(ffuns100));

ffun = resample(ffuns100,length(tmesh), length(ffuns100), 0);

V = zeros(length(xmesh), length(tmesh)+length(ffun)-1);
for ix=1:1:length(xmesh);
    V(ix,:)=(1e6)*dx*dt*conv(Green(ix,:), ffun, 'full')/tau/lambda;
end

figure;
surf(xmesh,tmesh(1:2:end/4),V(:,1:2:length(tmesh)/4)')
ylabel('Time (ms)');
xlabel('Displacement (um)');
zlabel('V(x,t) (uV)');
Title('Cable Equation Analytical Response: Sine(100Hz) Input in Spring
System');

ffuns250 = load('ffunsavs250');

ffuns250 = ffuns250.* (rlong*I0/max(ffuns250));

ffun = resample(ffuns250,length(tmesh), length(ffuns250), 0);

V = zeros(length(xmesh), length(tmesh)+length(ffun)-1);
for ix=1:1:length(xmesh);
    V(ix,:)=(1e6)*dx*dt*conv(Green(ix,:), ffun, 'full')/tau/lambda;
end
```

```
figure;
surf(xmesh,tmesh,V(:,1:1:length(tmesh))')
ylabel('Time (ms)');
xlabel('Displacement (um)');
zlabel('V(x,t) (uV)');
Title('Cable Equation Analytical Response: Sine(250Hz) Input in Spring
System');

ffuns375 = load('ffunsavs375');

ffuns375 = ffuns375.* (rlong*I0/max(ffuns375));

ffun = resample(ffuns375,length(tmesh), length(ffuns375), 0);

V = zeros(length(xmesh), length(tmesh)+length(ffun)-1);
for ix=1:1:length(xmesh);
    V(ix,:)=(1e6)*dx*dt*conv(Green(ix,:), ffun, 'full')/tau/lambda;
end

figure;
surf(xmesh,tmesh,V(:,1:1:length(tmesh))')
ylabel('Time (ms)');
xlabel('Displacement (um)');
zlabel('V(x,t) (uV)');
Title('Cable Equation Analytical Response: Sine(375Hz) Input in Spring
System');


% Numerical Solution to Spring Equation using ode23

t0 = 0;
tf = 1;
x0 = [0 0]';
[t,xvar] = ode23('Mech_Spring_fun',t0:tf,x0);
z = I_y(xvar(:,1));
save('ffunsavpulse', 'z', '-ascii');
plot(100*t,xvar(:,1))
hold on
plot(100*t,z, 'r')
Title('Spring System - ODE23 Response to Pulse Input');
xlabel('Time (ms)');
ylabel('Displacement (nm)');
hold off


function [Fout] = Mech_Spring_fun(t,x)
%SPRING_FUN Summary of this function goes here
%   Detailed explanation goes here

b = 4e-2;
K_s = 30e0;
M = 20e-3;
K_g = 6e-1;
m = 1e-3;
F0 = 200;
```

```
Fout = [x(2); (-1/m)*(K_g + K_s)*x(1)-b/m*x(2)+F0*(heaviside(t)-heaviside(t-
0.6))/m - M/m];

end


% Solution of the Cable Equation Using PDEPE
global rlong ;
global rmem ;
global cmem
global Vrest;
global Lcel;
global ffun;
global dt;
global dx;
global t_max;

dx=1;
dt=0.1;
x_min = 0;
x_max = 40;
t_max = 100;
I0 = 250e-12;

rlong = 1e7;
rmem = 8e10;
cmem = 5e-10;
Vrest = 0;
Lcel = x_max;
xmesh = x_min:dx:x_max;
tspan = 0:dt:t_max-dt;
options = odeset('InitialStep', 0.1, 'MaxStep', 0.1);


ffuntmp = load('ffunsavpulse');
ffuntmp = ffuntmp .*(I0/max(ffuntmp));
ffun = resample(ffuntmp,length(tspan), length(ffuntmp), 0);

m=0;
sol=pdepe(m,@cablepdefun,@cablepdeic,@cablepdebc,xmesh,tspan,options);
u= 100*sol(:,:,1);

figure;
surf(xmesh,tspan(1:2:end/4),u(1:2:length(tspan)/4,:))
Title('Cable Equation PDEPE Response: Pulse Input in Spring System');
ylabel('Time (ms)');
xlabel('Displacement (um)');
zlabel('V(x,t) (uV)');


ffuntmp = load('ffunsavs100');
ffuntmp = ffuntmp .*(I0/max(ffuntmp));
ffun = resample(ffuntmp,length(tspan), length(ffuntmp), 0);
```

```
m=0;
sol=pdepe(m,@cablepdefun,@cablepdeic,@cablepdebc,xmesh,tspan,options);
u= 100*sol(:,:,1);

figure;
surf(xmesh,tspan(1:2:end/4),u(1:2:length(tspan)/4,:))
Title('Cable Equation PDEPE Response: Sine(100Hz) Input in Spring System');
ylabel('Time (ms)');
xlabel('Displacement (um)');
zlabel('V(x,t) (uV)');

ffuntmp = load('ffunsavs250');
ffuntmp = ffuntmp .*(I0/max(ffuntmp));
ffun = resample(ffuntmp,length(tspan), length(ffuntmp), 0);

m=0;
sol=pdepe(m,@cablepdefun,@cablepdeic,@cablepdebc,xmesh,tspan,options);
u= 100*sol(:,:,1);

figure;
surf(xmesh,tspan,u)
Title('Cable Equation PDEPE Response: Sine(250Hz) Input in Spring System');
ylabel('Time (ms)');
xlabel('Displacement (um)');
zlabel('V(x,t) (uV)');

ffuntmp = load('ffunsavs375');
ffuntmp = ffuntmp .*(I0/max(ffuntmp));
ffun = resample(ffuntmp,length(tspan), length(ffuntmp), 0);

m=0;
sol=pdepe(m,@cablepdefun,@cablepdeic,@cablepdebc,xmesh,tspan,options);
u= 100*sol(:,:,1);

figure;
surf(xmesh,tspan,u)
Title('Cable Equation PDEPE Response: Sine(375Hz) Input in Spring System');
ylabel('Time (ms)');
xlabel('Displacement (um)');
zlabel('V(x,t) (uV)');

function [ c,f,s ] = cablepdefun( x,t,v,DvDx )
global rlong ;
global rmem ;
global cmem ;
global dt;
global dx;
global ffun;

   if x == 0.5*dx
      z = ffun(floor((t+dt)/dt));
   else
       z=0;
   end
```

```
c=cmem;
f=(1/rlong)*DvDx;
s= -v/rmem + z;
return
end



function [ pl, ql,pr,qr ] = cablepdebc( xl,ul,xr,ur,t )
global rlong ;
global rmem ;
global cmem ;
global Vrest;
global Lcel;
pl=0;
ql=rlong;
pr=0;
qr=rlong;
return
end



function [ V0 ] = cablepdeic( x )
global rlong ;
global rmem ;
global cmem ;
global Vrest;
global Lcel;

V0=Vrest;
end
```